Quantitative Study on Error Sensitivity in Ultrasound Probe Calibration with Hybrid Tracking

Qianqian Cai
Department of Mechanical and Aerospace Engineering
North Carolina State University
Raleigh, NC, United States
qcai2@ncsu.edu

Tianfu Wu
Department of Electrical and Computer Engineering
North Carolina State University
Raleigh, NC, United States
twu19@ncsu.edu

Jian-yu Lu
Department of Bioengineering
The University of Toledo
Toledo, OH, United States
jian-yu.lu@ieee.org

Juan C. Prieto
Division of Global Health, Department of Obstetrics and Gynecology
University of North Carolina - Chapel Hill
Chapel Hill, NC, United States
juan_prieto@med.unc.edu

Alan J. Rosenbaum
Division of Global Health, Department of Obstetrics and Gynecology
University of North Carolina - Chapel Hill
Chapel Hill, NC, United States
alan_rosenbaum@med.unc.edu

Jeffrey S. A. Stringer
Division of Global Health, Department of Obstetrics and Gynecology
University of North Carolina - Chapel Hill
Chapel Hill, NC, United States
jeffrey_stringer@med.unc.edu

Xiaoning Jiang
Department of Mechanical and Aerospace Engineering
North Carolina State University
Raleigh, NC, United States
xjiang5@ncsu.edu

***Abstract*— Three-dimensional (3D) freehand ultrasound (US) imaging enabled by the external tracking system requires an accurate calibration process to transform the tracked motion information from the markers to the US frames. The previously proposed phantomless calibration method can be further improved using both optical tracking and image-based tracking. This study provides a quantitative analysis on the error sensitivity before implementing the image-based tracking during the calibration process. A linear relationship was found between the perturbation in imaging plane motion estimation and the error caused in the calibration solution. The error to perturbation ratio was within 0.5 in most cases and can reach up to around 0.9 in some poor cases. The overall analysis showed a good error tolerance for the hybrid tracking enabled US probe calibration.**

Keywords—3D freehand ultrasound, spatial calibration, error sensitivity

I. Introduction

Freehand three-dimensional ultrasound imaging is considered as a cost-efficient imaging technique enabled by external tracking of the probe to resolve the experience dependence of conventional ultrasound imaging, and provide an intuitive and measurable volume reconstruction at the meanwhile [1]. To achieve accurate 3D reconstruction from a series of US frames, a calibration step should be conducted to transfer the tracked trajectory relative to the markers of the tracking system to US frames themselves [2]. Majority of current probe calibration methods require phantom imaging to estimate the transformation matrix. Although it is accurate and requires less computational load, such methods require designed and fabricated phantoms, and the imaging as well as the segmentation of the intersectional imaging from the US frames can be time-consuming and challenging. Thus, these methods are hard to translated to routine clinical practice.

A phantomless calibration method was proposed based on general motion of the US probe [3]. To numerically solve the unknown calibration matrix T_X, general probe motions should be tracked to obtain the relative motion of the marker set attached to the top of the probe (T_A) and the imaging plane (T_B). As shown in Fig. 1, the unknown parameters can be solved based on the equation $T_A T_X = T_X T_B$. At least two independent general motions that do not share parallel axes are necessary to solve the equation uniquely. The previous method utilized a marker-set to capture the trajectory of the imaging plane during the calibration step. Although the marker-set can be detached from the probe after calibration, this method still requires additional imaging test to make sure the markers all lie in the imaging plane to ensure the tracking accuracy.

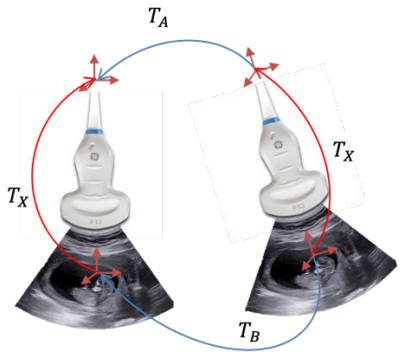

Fig. 1. Schematic of estimating the calibration matrix using the relative motions of the marker-set attached to the top of the US probe and the imaging plane

To further adapt such method into a clinical practice, an image-based tracking can be a substitute for the bottom marker-set to estimate the relative imaging plane motion based on the frames obtain in the calibration. T_A is the relative motion of the marker-set attached to the probe and that marker-set is attached

2021 IEEE International Ultrasonics Symposium Proceedings
DOI: 10.1109/IUS52206.2021.9593708. 978-0-7381-1209-1/21/$31.00@2021 IEEE

during the whole exam for the tracking purpose. The hybrid tracking enabled calibration takes advantages of the accuracy and precision of the optical tracking and also has the advantage of the image-based motion tracking from the patient US frames, without need of additional phantoms. The occlusion issue of optical tracking can also be resolved using a hemispherical marker rigid body [4]. Integrated with the optical tracking system, the proposed calibration will only take minutes to obtain the data for image-based motion tracking, thus the computational load will be greatly reduced compared with learning-based sensorless 3D freehand ultrasound. However, compared with the optical tracking, the image-based motion tracking in US frames is very challenging especially along the elevational direction [5].

In this work, we conducted a quantitative study on the error sensitivity of previously proposed calibration method before utilizing the hybrid tracking strategy for enabling accurate and clinical-friendly probe calibration and tracking. The goal is to analyze the significant error range in estimating the imaging plane motion, both in position and orientation. Such error tolerance will help us establish the goal towards image-based motion tracking based on US frames in the hybrid tracking.

II. Methods

A. Data Collection

The testing dataset was obtained with two marker-sets attached on the portable Butterfly iQ probe (Butterfly Network, Guilford, CT, USA) as shown in Fig. 2, where the trajectories of each marker-set were recorded by the optical tracking system OptiTrack V120: Trio (NaturalPoint, Inc.). The sampling rate of tracking was 100 Hz. The reference coordinate system fixed on the optical tracking system followed the right-hand rule with the y-axis pointing upwards. The coordinate system is presented in Fig. 3. According to the previous study [6], the tracking accuracy can achieve submillimeter for positional tracking and arcsecond degree level for orientational tracking.

To generate the tracking information of two independent general motions, the probe was held by hand and moved from different starting positions to end positions with different orientations. At each pose, the probe was held still for about one second to collect enough motion data.

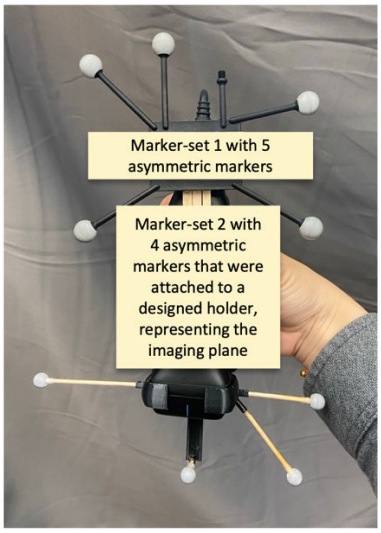

Fig. 2. Data collection of probe calibration with two marker-sets rigidly attached to the US probe

For each motion with a starting pose and ending pose, a pair of coefficient matrices T_A and T_B could be derived from the trajectory tracked by the optical camera. Thus, the calibration matrix T_X can be solved numerically through the matrix equation $T_A T_X = T_X T_B$. To further minimize the calibration error in the process of numerically solving the matrix equation, an iterative optimization based on the genetic algorithm was applied after obtaining the solution. Meanwhile, the connection between the probe and the marker sets is rigid. And the spatial relationship between the upper marker set and the imaging plane is constant. Thus, the ground truth of the calibration matrix T_X can be calculated from the tracked marker sets by taking the inverse operation $T_X = {T_U}^{-1} T_L$ as indicated in Fig. 3. By comparing the estimated calibration matrix with the ground truth, the error was obtained and considered as the reference to evaluate the performance when introducing perturbation to the estimated imaging plane motion. The reference performance is presented in Section III A.

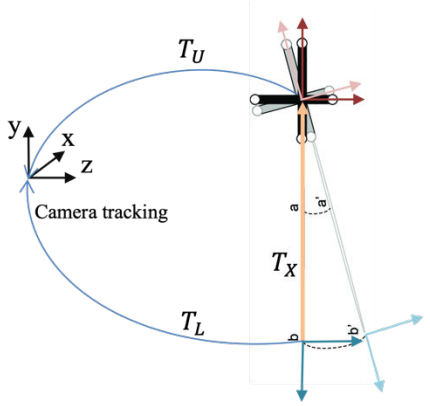

Fig. 3. Schematic for solving the ground truth of the calibration matrix with the tracked marker-sets

B. Simulation on Error Sensitivity

The work was supported by Bill & Melinda Gates Foundation under the Award OPP1191684.

The transformation matrices are composed of 6 degree-of-freedom (DoF) in the relative spatial relationship between two coordinates. To simulate the error of the image-based tracking of relative imaging plane motion, certain range of perturbation was applied on all the 6 DoF in the estimated matrix T_B. Based on the averaged range of tracking accuracy reported in recent learning-based tracking using the generated 2D US frames, perturbations from -5 mm to 5 mm and from -5° to 5° were applied to each degree of the positional and orientational tracking of the relative imaging plane motion, respectively. Theoretically, as the matrix T_B cannot accurately describe the relative imaging plane motion, the estimated transformation matrix T_X calculated from T_A and T_B will deviate from the ground truth that is determined based on the geometric design of the US probe integrated with the attached marker-set.

III. Results and Discussion

A. Calibration Error with Two Marker-Sets Attached

Two pairs of starting pose and ending pose were selected from the probe trajectory. The data was further averaged to get rid of the measurement noise. In addition, two pairs of coefficient matrices T_{A1}, T_{B1} and T_{A2}, T_{A2} were obtained to numerically solve the transformation matrix T_X based on the closed-form solution provided in [7]. To compare the results with the ground truth intuitively, the 4×4 transformation matrix was converted to the 6 DoF representing the orientation and translation of one coordinate system (the coordinate attached to the marker-set before the motion) with respect to the other coordinate system (the coordinate attached to the marker-set after the motion). The absolute errors are shown in Table I.

To further improve the calibration accuracy, an iterative optimization was conducted with the objective function to be

$$T_X = min \, \|T_A T_X - T_X T_B\| \quad (1)$$

The optimized results were also evaluated with the absolute error and shown in Table I, where T_X was the calculated transformation matrix from the equation and $T_{X_{opti}}$ was obtained via the optimization step. As the error analysis indicates, the optimization improved the calibration performance to submillimeter level for position and subdegree level for orientation. The calibration accuracy is comparable to recently reported performance in [8]–[10] using both phantom-based and phantomless calibration method, where the relative imaging plane motion was tracked by the optical tracking system.

TABLE I. Error Analysis with Two Marker-Sets Probe Calibration

	Roll (°)	Yaw (°)	Pitch (°)	X (mm)	Y (mm)	Z (mm)
T_X	1.81	2.15	2.32	2.32	2.64	9.75
$T_{X_{opti}}$	0.72	0.30	0.15	1.00	1.38	0.25

B. Analysis on Error Sensitivity

Compared with external tracking systems, image-based position tracking comes with less hardware dependency but with lower accuracy and precision. As reported in the recent published works [11], [12], the tracked motion had a distance error of around 10 mm on average using EM tracking and the error of orientational measurement was about a few degrees. Therefore, a 10 mm perturbation ranges from -5 mm to 5 mm and orientational perturbation from -5° to 5° were introduced to each degree of T_B in the error simulation to study its effect on each degree of T_X. In total, 36 analyses were carried out to evaluate the error sensitivity. Three of them were reported to demonstrate the relationship found between the perturbation in each degree of T_B and the error caused in the calibration solution, as well as to offer a complete view of the analysis.

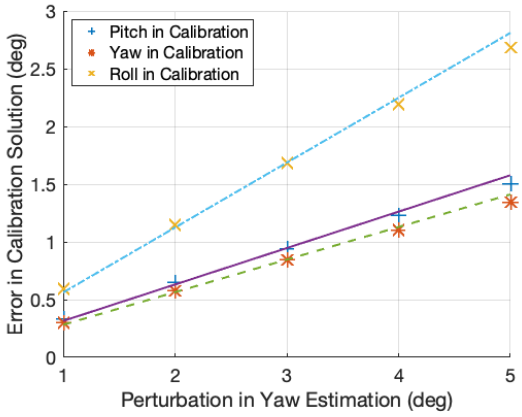

Fig. 4. Median case: the error to perturbation ratio is around or within 0.5

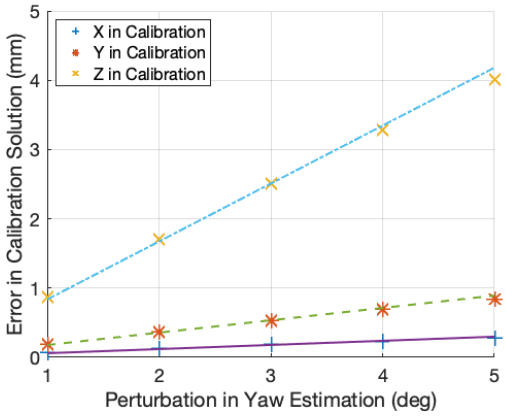

Fig. 5. Poor case 1: the perturbation in the orientation estimation in T_B has larger impact on positional error caused in T_X.

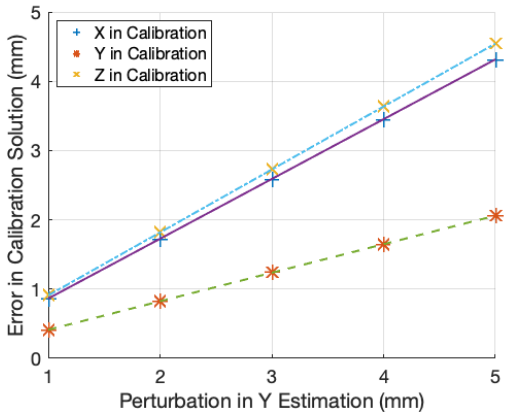

Fig. 6. Poor case 1: the perturbation in the positional estimation in T_B has larger impact on orientational error caused in T_X.

It is noticed that the error sensitivity analysis can vary based on different geometric configuration. In this case, Fig. 4 shows the median case of the entire analysis, where a clear linear relationship could be found between the perturbation and the caused error in calibration matrix. In addition, the error to perturbation ratio was represented by the slope. In a median case, the slope ranged from 0.3 to 0.6, which demonstrates a good error tolerance performance. Fig. 5 and Fig. 6 were selected to offer a view of the poor cases, where the slope varied up to around 0.9. Overall, the quantitative error analysis of the proposed calibration method shows a great error tolerance for the future image-based probe calibration. A published work can already successfully classify and segment the fetal ultrasound images [13]. Based on these findings, our future work includes training the learning-based network to track the relative imaging plane motion and verify the calibration results with existing phantom-based calibration methods.

IV. Conclusion

This paper reported the quantitative analysis on the error sensitivity in a close-form solution of ultrasound probe calibration for future hybrid tracking enabled probe calibration. In this study, a range of perturbation was introduced to the estimated imaging plane motion. And the calibration matrix was solved with the disturbed estimation. All the transformation matrices were converted to the 6 degree-of-freedom to intuitively compare the performance. A linear relationship was found between the perturbation and the resulted errors. Further, the error to perturbation ratio was within 0.5 for most cases and can reach up to around 0.9, which indicates a good error tolerance for future hybrid tracking enabled calibration using the image-based imaging plane motion tracking during the calibration process.

Acknowledgment

The work was supported by Bill & Melinda Gates Foundation under the Award OPP1191684. The authors would like to thank Butterfly Network, Guilford, CT, USA for providing the Butterfly iQ probe.

References

[1] M. H. Mozaffari and W.-S. Lee, “Freehand 3-D Ultrasound Imaging: A Systematic Review,” *Ultrasound in Medicine and Biology*, vol. 43, no. 10, pp. 2099–2124, Oct. 2017, doi: 10.1016/j.ultrasmedbio.2017.06.009.

[2] L. Mercier, T. Langø, F. Lindseth, and L. D. Collins, “A review of calibration techniques for freehand 3-D ultrasound systems,” *Ultrasound in Medicine & Biology*, vol. 31, no. 2, pp. 143–165, Feb. 2005, doi: 10.1016/j.ultrasmedbio.2004.11.001.

[3] Q. Cai *et al.*, “Spatial Calibration for 3D Freehand Ultrasound via Independent General Motions,” in *2020 IEEE International Ultrasonics Symposium (IUS)*, Las Vegas, NV, USA, Sep. 2020, pp. 1–3. doi: 10.1109/IUS46767.2020.9251558.

[4] Q. Cai *et al.*, “Performance Enhanced Ultrasound Probe Tracking With a Hemispherical Marker Rigid Body,” *IEEE Transactions on Ultrasonics, Ferroelectrics, and Frequency Control*, vol. 68, no. 6, pp. 2155–2163, Jun. 2021, doi: 10.1109/TUFFC.2021.3058145.

[5] A. H. Gee, R. James Housden, P. Hassenpflug, G. M. Treece, and R. W. Prager, “Sensorless freehand 3D ultrasound in real tissue: Speckle decorrelation without fully developed speckle,” *Medical Image Analysis*, vol. 10, no. 2, pp. 137–149, Apr. 2006, doi: 10.1016/j.media.2005.08.001.

[6] Q. Cai, C. Peng, J. Prieto, A. Rosenbaum, J. Stringer, and X. Jiang, *A Low-Cost Camera-Based Ultrasound Probe Tracking System: Design and Prototype*. 2019. doi: 10.1109/ULTSYM.2019.8925631.

[7] Y. C. Shiu and S. Ahmad, “Calibration of wrist-mounted robotic sensors by solving homogeneous transform equations of the form AX=XB,” *IEEE Transactions on Robotics and Automation*, vol. 5, no. 1, pp. 16–29, Feb. 1989, doi: 10.1109/70.88014.

[8] Y. Lin, Z. Wang, X. Guo, H. Wang, and F. Wang, “Closed-form freehand 3D ultrasound spatial calibration based on N-wedge phantom,” Art. no. 426, Aug. 2018, doi: 10.29007/zrzd.

[9] M. Toews and W. M. Wells, “Phantomless Auto-Calibration and Online Calibration Assessment for a Tracked Freehand 2-D Ultrasound Probe,” *IEEE Transactions on Medical Imaging*, vol. 37, no. 1, pp. 262–272, Jan. 2018, doi: 10.1109/TMI.2017.2750978.

[10] C. Shen, L. Lyu, G. Wang, and J. Wu, “A method for ultrasound probe calibration based on arbitrary wire phantom,” *Cogent Engineering*, vol. 6, no. 1, p. 1592739, Jan. 2019, doi: 10.1080/23311916.2019.1592739.

[11] R. Prevost *et al.*, “3D freehand ultrasound without external tracking using deep learning,” *Medical Image Analysis*, vol. 48, pp. 187–202, Aug. 2018, doi: 10.1016/j.media.2018.06.003.

[12] H. Guo, S. Xu, B. Wood, and P. Yan, “Sensorless Freehand 3D Ultrasound Reconstruction via Deep Contextual Learning,” *arXiv:2006.07694 [cs, eess]*, Jun. 2020, Accessed: Jun. 16, 2021. [Online]. Available: http://arxiv.org/abs/2006.07694

[13] J. C. Prieto *et al.*, “An automated framework for image classification and segmentation of fetal ultrasound images for gestational age estimation,” in *Medical Imaging 2021: Image Processing*, Feb. 2021, vol. 11596, pp. 453–462. doi: 10.1117/12.2582243.